Supplementary Information

Casein Kinase II is Required for Proper Cell Division and Acts as a Negative Regulator of Centrosome Duplication in *C. elegans* Embryos

Jeffrey C. Medley[1], Megan M. Kabara[1], Michael D. Stubenvoll[1], Lauren E. DeMeyer[1], and Mi Hye Song[1,2]

[1]Department of Biological Sciences, Oakland University, Rochester, MI 48309, USA.

[2]To whom correspondence should be addressed.

Contact Information: msong2@oakland.edu

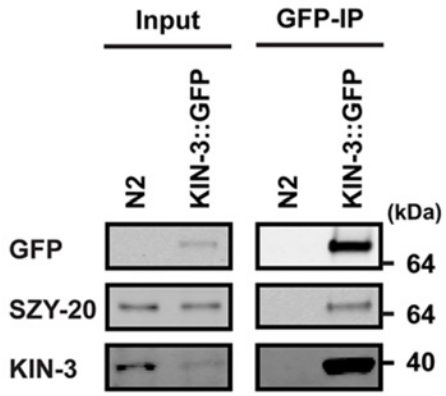

Figure S1. KIN-3/CK2α, the catalytic subunit of CK2, physically interacts with SZY-20 in *C. elegans* embryos. SZY-20 co-precipitates with KIN-3::GFP. Protein lysates from wild-type (*N2*) embryos were used as a negative control. ~5% of total embryonic lysates were loaded in input lanes. While endogenous SZY-20 levels are similar between two samples in input lanes, endogenous KIN-3 levels are much lower in embryos expressing KIN-3::GFP compared to KIN-3 levels in wild-type (*N2*), suggesting that the transgene expression of KIN-3::GFP is likely to down-regulate endogenous KIN-3 expression. However, endogenous KIN-3 co-precipitates with KIN-3::GFP (IP lane), suggesting KIN-3::GFP physically interacts with endogenous KIN-3.

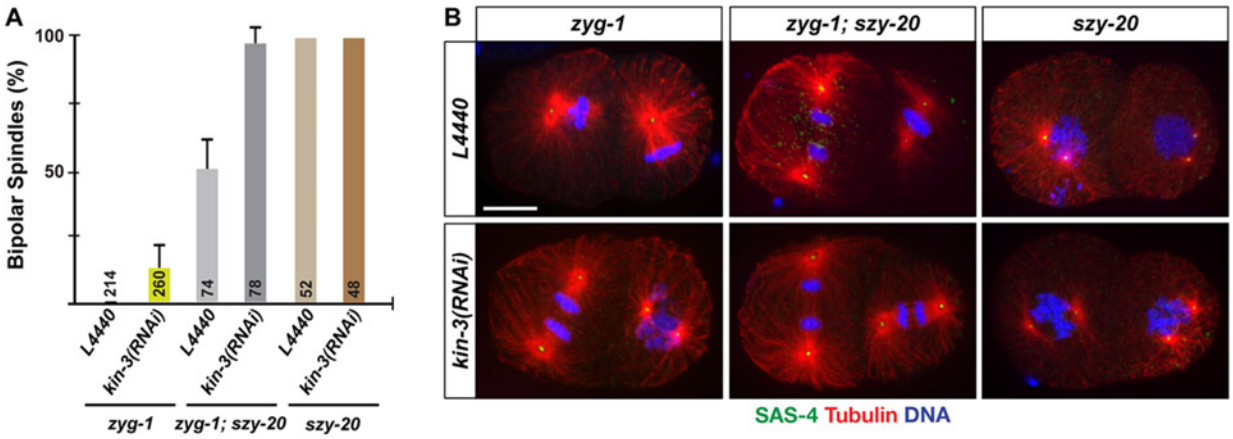

Figure S2. Co-depleting KIN-3 and SZY-20 further enhances bipolar spindle formations to *zyg-1(it25)* embryos. (A) Quantification of bipolar spindle formation in *zyg-1(it25), zyg-1(it25); szy-20(bs52)* and *szy-20(bs52)* embryos treated with *kin-3(RNAi)* and control RNAi (*L4440)* at 24ºC, the restrictive temperature for *zyg-1(it25)* (O'Connell et al., 2001; Song et al., 2008). *kin-3(RNAi)* in *zyg-1(it25);szy-20(bs52)* double mutants further increases (95.8 ± 5.9%) bipolar spindle formation, compared to a partial restoration of bipolar spindle formation to *zyg-1(it25)* by *kin-3(RNAi)* (12.9 ± 8.4%) or *szy-20(bs52)* (49.3 ± 11.5%) alone. n is given as the number of blastomeres scored. Average values are shown. Error bars are s.d. (B) Immunostained embryos illustrate monopolar or bipolar spindles at the second mitosis. For example, both blastomeres in the *kin-3(RNAi)* treated *zyg-1(it25)* embryo show bipolar spindles. In contrast, the control RNAi treated *zyg-1(it25)* embryo exhibit monopolar spindles in both although the cell cycle is more progressed in P1 (right) compared to that of the *kin-3(RNAi);zyg-1(it25)* embryo . Scale bar, 10 µm.

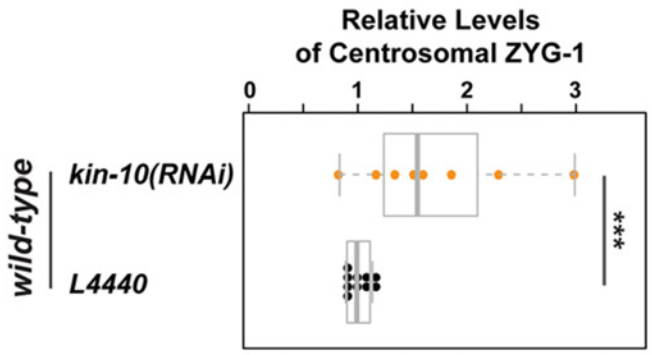

Figure S3. Knocking down KIN-10/CK2β, the regulatory subunit of CK2, leads to increased ZYG-1 levels at centrosomes. Centrosomal ZYG-1 levels at first anaphase were quantified in wild-type embryos treated with *kin-10(RNAi)* or control (*L4440)*. Values are relative to centrosomal ZYG-1 levels in wild-type embryos treated with control. *kin-10(RNAi)* results in an increase in centrosomal ZYG-1 (1.70 ± 0.41 fold). Each dot represents a centrosome. Box ranges from the first through third quartile of the data, and thick bar represents the median. Dashed line extends 1.5 times the inter-quartile range or to the minimum and maximum data point. ****p*<0.001 (two-tailed t-test).

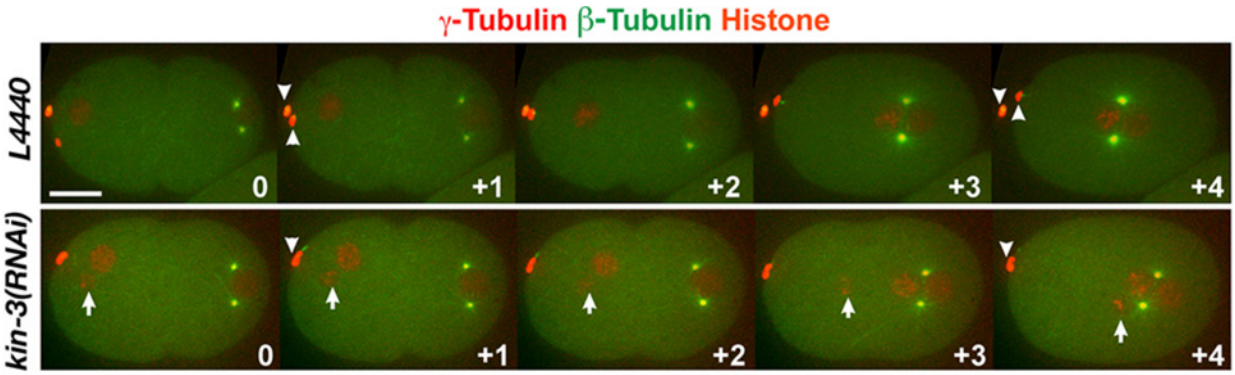

Figure S4. Defective meiotic divisions are observed in *kin-3(RNAi).* Shown are still images selected from 60 sec-interval 4D time-lapse movies. *kin-3(RNAi)* results in an error in meiotic division, likely leading to extra DNA (arrows). While control embryo exhibits two polar bodies (arrowheads), *kin-3(RNAi)* embryo shows only one polar body. Although we cannot rule out the possibility that the second polar body is out of focus in this movie, it is also possible that KIN-3 depletion may lead to polar body extrusion failure and extra DNA. Time is given relative to the start of the movie (end of the second meiotic division). Scale bar, 10 µm**.**

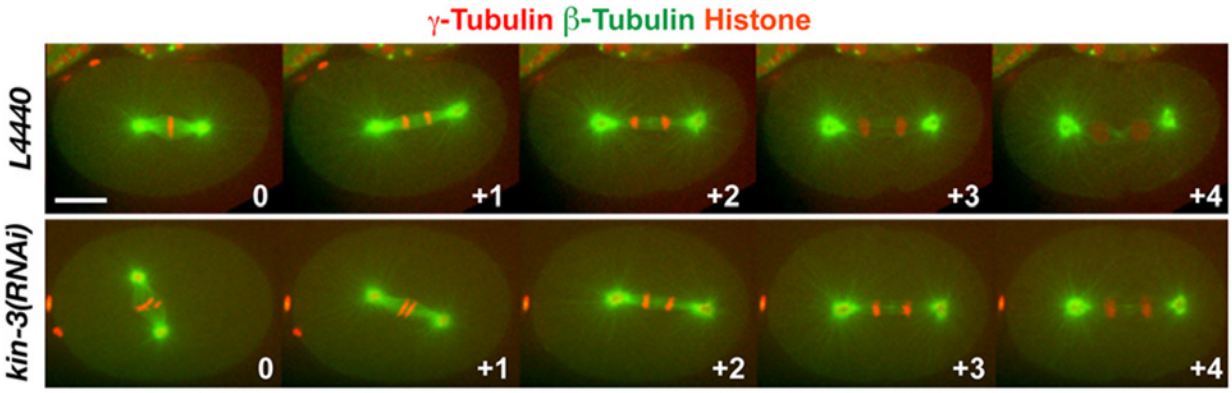

Figure S5. *kin-3(RNAi)* leads to a delay in cell cycle progression Shown are still images selected from 60 sec-interval 4D time-lapse movies of *kin-3(RNAi)* (n=48 embryos) or control RNAi (n=42 embryos). While the control embryo progresses from metaphase (t=0) to telophase (t=+4) during the shown time interval, the *kin-3(RNAi)* embryo progresses from metaphase (t=0) to anaphase (t=+4) during the same time interval. Time (min) is relative to the first metaphase. Scale bar, 10 µm.

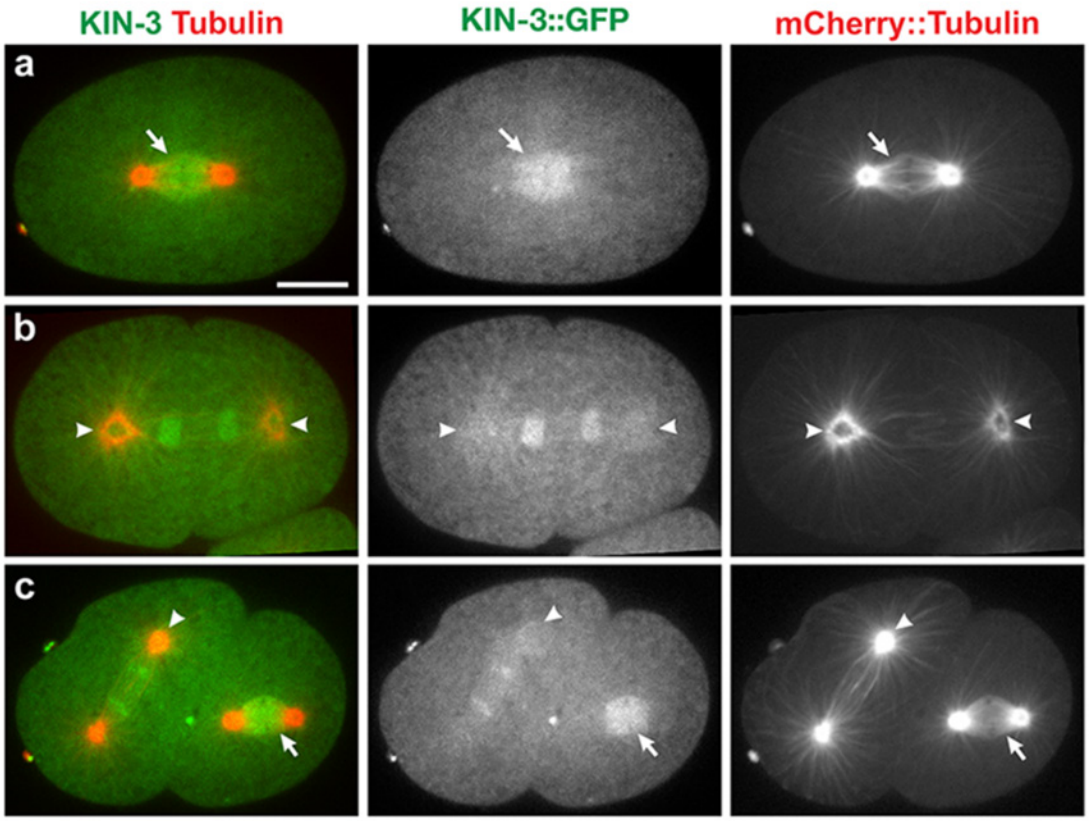

Figure S6. KIN-3 localizes to the mitotic spindle and centrosomes. KIN-3::GFP co-localizes with mCherry::Tubulin at spindle microtubules (arrows) at the first (a) and second (c) metaphase. During late mitosis in the first (b) and second (c) cell division, KIN-3::GFP appears to be associated with centrosomes (arrowheads) that are highlighted with mCherry::Tubulin co-localization. Shown are still images selected from 4D time-lapse movies. Scale bar, 10 µm.

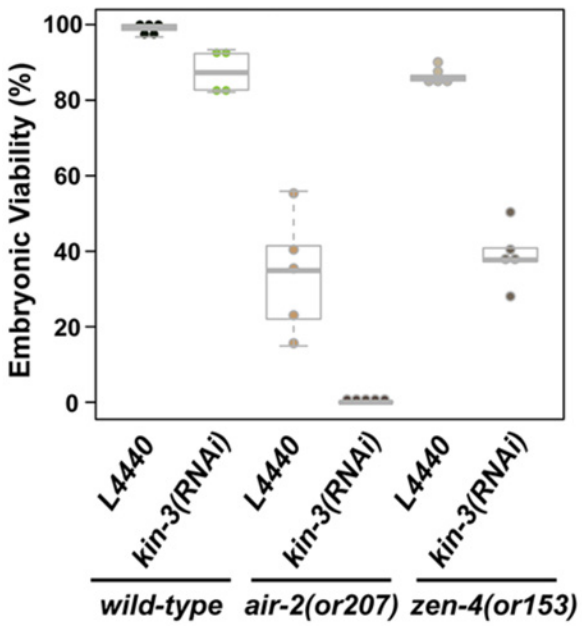

Figure S7. Depleting KIN-3 further decreases embryonic viability in *air-2(or207)* and *zen-4(or153)* mutants. At 17ºC, *kin-3(RNAi)* in wild-type worms (n=605) produces 87.5% (± 5.6) embryonic viability and *air-2(or207ts)* mutants (n=672) exhibit 33.0% (± 16.0) embryonic viability. In contrast, *kin-3(RNAi)* in *air-2(or207)* mutants (n=819) leads to 0.3% (± 0.6) embryonic viability, which suggests a positive genetic interaction between *kin-3* and *air-2.* Similarly, *zen-4(or153)* mutants (n=740) exhibit 86.7% (± 2.4) embryonic viability, whereas *kin-3(RNAi)* in *zen-4(or153)* mutants (n=797) leads to 39.0% (± 8.4) embryonic viability at 17ºC, showing decreased embryonic viability by co-depleting *kin-3* and *zen-4*. Each dot marks % embryonic viability of the progeny produced by a single worm (n=the total number of progeny scored). Boxes range from the first through third quartile of the data and thick bars represent the median. Dashed lines extend 1.5 times the inter-quartile range, or to the minimum and maximum data point.

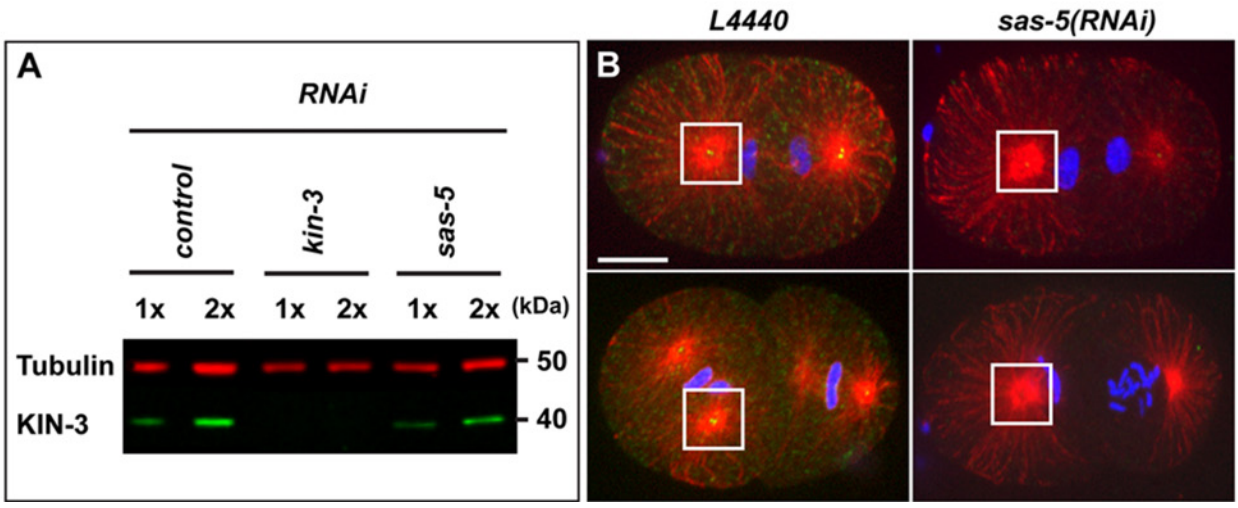

Figure S8. Antibody specificity (A) Immunoblot illustrates that anti-KIN-3 detects endogenous KIN-3 in control and *sas-5(RNAi)* embryos but detection is abolished by *kin-3(RNAi)*, suggesting the specificity of KIN-3 antibody. Tubulin was used as a loading control. (B) SAS-5 antibodies detect SAS-5 at centrosomes and cytoplasm. However, *sas-5(RNAi)* significantly diminishes SAS-5 detection, indicating the antibody specificity. Boxes highlight centrosomes. Scale bar, 10 µm.

Table S1. Mass spectrometry analysis

Lysates	Antibody	Protein	Peptides	Coverage (%)	Peptide sequences
N2	α-SZY-20	KIN-3	5	11.0	GGTNIITLLDVVK LIDWGLAEFYHPR VLGTDELYEYIAR
KIN-3::GFP	α-GFP	KIN-10	2	5.1	FNLTGLNEQVPK
		SZY-20	5	10.4	VKAEESSGVVSK LQTEEGLGPSAEEPKR LQTEEGLGPSAEEPK MTQQNMVEHYGEELSR ELMEQPAEIVPPER
		ZEN-4	4	6.5	VFSENDGQATVFER TLDVIFNSINNR GIIDNPSPSVASLR VPTGTVLQSR
		CYK-4	3	5.3	LDLNVYETR TVNVLLDELR SILGPVTTSPATPLLAR
		ICP-1	6	15.0	ISSIFDEVSEAHDDAAAK IDAEFVELISR VEILIGSDGQK TAPVAQPTVELSPSR AHAASSSTSNVEAAAALAALQEQQR DVPAWAEFAVVR
		PLK-1	15	23.6	IGDFGLATTVNGDER SLEETYSR HNNYTIPSIATQPAASLIR SGFMPTR FGGHETSMMEENVAPR AGLSALPQHIVSNNADRER IMLDQAGNELTYIEK SYMNDHLVK LMSDANVVSQNPAR GPNQAASHLPQSASGSNIHPR KAVTEPEAR

Selected proteins identified by mass spectrometry following immunoprecipitation (IP) of embryonic lysates from wild-type using anti-SZY-20 (Song et al., 2008), and a strain expressing KIN-3::GFP using anti-GFP (MBL, Naka-ku, Nagoya, Japan). Mass spectrometry was performed as described (Song et al., 2011). The total number of peptides identified by mass spectrometry is listed for each protein. Sequence coverage is the total number of identified amino acid residues out of the total number of amino acid residues for each protein. For proteins with multiple isoforms, sequence coverage is based on the largest isoform listed at wormbase.org. SZY-20 co-precipitated with KIN-3/CK2α that also pulled down KIN-10/CK2β. In

total, our mass spectrometry analysis following IP assay identified 198 proteins that co-precipitated with KIN-3::GFP with at least two unique peptides and 5% coverage. We detected several known midbody components (ZEN-4, CYK-4, ICP-1 and PLK-1) in KIN-3::GFP co-precipitates, suggesting a role of KIN-3 as part of the midbody structure.

Table S2. Genetic Analysis of CK2

	°C	% Embryonic Viability (ave ± s.d.)	n
N2; L4440	24.0[a]	98.5 ± 1.2	3190
N2; kin-3(RNAi)		55.7 ± 16.1	3724
N2; kin-10(RNAi)		77.4 ± 7.0	1147
zyg-1(it25); L4440		0.2 ± 1.0	1090
zyg-1(it25); kin-3(RNAi)		0.4 ± 1.2	1078
zyg-1(it25); kin-10(RNAi)		0.6 ± 1.0	576
szy-20(bs52); L4440		29.1 ± 22.3	163
szy-20(bs52); kin-3(RNAi)		27.6 ± 15.8	238
zyg-1(it25); szy-20(bs52); L4440		17.8 ± 24.6	183
zyg-1(it25); szy-20(bs52); kin-3(RNAi)		13.9 ± 20.1	382
N2; L4440	22.5[a]	98.5 ± 1.4	2921
N2; kin-3(RNAi)		52.8 ± 10.4	2433
N2; kin-10(RNAi)		55.0 ± 20.5	1268
zyg-1(it25); L4440		8.0 ± 12.6	7257
zyg-1(it25); kin-3(RNAi)		24.8 ± 24.9	7389
zyg-1(it25); kin-10(RNAi)		40.3 ± 26.1	2786
N2; DMSO	22.5[b]	96.2 ± 2.0	276
N2; 15μM TBB		96.9 ± 8.1	174
zyg-1(it25); DMSO		3.1 ± 3.1	637
zyg-1(it25); 15μM TBB		37.0 ± 21.8	330
N2; L4440	17.0[c]	98.9 ± 1.3	702
N2; kin-3(RNAi)		87.5 ± 5.6	605
air-2(or207); L4440		33.8 ± 16.1	672
air-2(or207); kin-3(RNAi)		0.3 ± 0.6	819
zen-4(or153); L4440		86.7 ± 2.4	740
zen-4(or153); kin-3(RNAi)		38.8 ± 8.4	797

[a]: Presented in Fig. 1
[b]: Presented in Fig. 6
[c]: Presented in Fig. S5

Table S3. List of *C. elegans* strains used in this study

Name	Genotype	Origin
N2	*wild-type*	CGC
OC14	*zyg-1(it25) II*	Kemphues et al., 1988
OC133	*szy-20(bs52) II*	Song et al., 2008
OC95	*bsIs2[pie-1p::GFP::spd-2 + unc-119(+)]; ruIs32[pie-1p::GFP::his-58 + unc-119(+)] III.*	Kemp et al., 2004
OC341	*unc-119(ed3) III; bsIs8[pMS5.1:unc-119(+) pie-1p::GFP::zyg-1C-terminus]*	Peters et al., 2010
OC481	*unc-119(ed3) III; bsIs15[pNP99:unc-119(+) tbb-1p::mCherry::tbb-2::tbb-2 3'UTR*	Gift from O'Connell Lab
EU630	*air-2(or207) I*	Severson et al., 2000
EU716	*zen-4(or153) IV*	Severson et al., 2000
OD70	*unc-119(ed3) III; ltIs44 [pie-1p-mCherry::PH(PLC1delta1) + unc-119(+)] V*	Kachur et al., 2008
SA250	*tjIs54[pie-1p::GFP::tbb-2 + pie-1p::2xmCherry::tbg-1 + unc-119(+)]; tjIs57[pie-1p::mCherry::his-48 + unc-119(+)]*	Toya et al., 2010
MTU5	*unc-119(ed3) III; [kin-3p::kin-3::gfp::3xflag::kin-3 3'UTR + unc-119(+)]*	This study; Sarov et al., 2012